



ELSEVIER

Available online at [www.sciencedirect.com](http://www.sciencedirect.com)

SCIENCE @ DIRECT®

Optics Communications 234 (2004) 337–342

OPTICS  
COMMUNICATIONS

[www.elsevier.com/locate/optcom](http://www.elsevier.com/locate/optcom)

# High-power efficient diode-pumped passively Q-switched Nd:YVO<sub>4</sub>/KTP/Cr<sup>4+</sup>:YAG eye-safe laser

Y.F. Chen \*, Y.C. Chen, S.W. Chen, Y.P. Lan

*Department of Electrophysics, National Chiao Tung University, 1001 TA Hsueh Road, Hsinchu 30050, Taiwan*

Received 22 September 2003; received in revised form 6 January 2004; accepted 6 February 2004

## Abstract

A high-power efficient eye-safe laser is experimentally realized by using an intracavity optical parametric oscillators of a diode-pumped passively Q-switched Nd:YVO<sub>4</sub>/Cr<sup>4+</sup>:YAG laser. Considering the thermal lensing effects, the cavity length was designed to allow mode matching with the pump beam and to provide the proper spot size in the saturable absorber. With an incident pump power of 14.5 W, the compact intracavity OPO cavity, operating at 58.5 kHz, produces average powers at 1573 nm up to 1.56 W and peak powers higher than 5 kW.

© 2004 Elsevier B.V. All rights reserved.

PACS: 42.60.Gd; 42.65.Yj; 42.55.Xi

Keywords: Diode-pumped; Eye-safe; Q-switched

## 1. Introduction

Nanosecond pulsed lasers at the eye-safe wavelength region (1.5–1.6 μm) are indispensable to applications such as telemetry and range finders [1]. Laser emission at this spectral range has been reported from several gain materials including Co:MgF<sub>2</sub> [2], Ni:MgF<sub>2</sub> [3], Cr<sup>4+</sup>:YAG [4,5], Er<sup>3+</sup>:YLiF<sub>4</sub> [6], Er<sup>3+</sup>:KY(WO<sub>4</sub>)<sub>2</sub> [7], Er<sup>3+</sup>:YVO<sub>4</sub> [8], Yb<sup>3+</sup>:Tm<sup>3+</sup>:YLiF<sub>4</sub> [9] and Er:Yb:glass [10]. Pulsed operation near 1.55 μm has been achieved with passive Q-switching by use of Co<sup>2+</sup>:LaMg-

Al<sub>11</sub>O<sub>19</sub> [11], Er:Ca<sub>5</sub>(PO<sub>4</sub>)<sub>3</sub>F [12], U<sup>4+</sup>:CaF<sub>2</sub> [13], U<sup>4+</sup>:SrF<sub>2</sub> [14], Co<sup>2+</sup>:ZnSe [15], Cr<sup>2+</sup>:ZnSe [16] or a semiconductor saturable absorber mirror (SESAM) [17]. Another approach for high-peak-power eye-safe laser sources is based on intracavity optical parametric oscillators (OPO's) [18]. Recently, there has been a resurgence of interest in intracavity OPO's, as their merits have been appreciated with the advent of high-damage-threshold nonlinear crystals and diode-pumped Nd-doped lasers [19–21].

Diode-pumped Q-switched Nd-doped lasers are compact efficient solid-state lasers. In recent year, Cr<sup>4+</sup>:YAG crystals have been successfully used as passive Q-switches for a variety of gain media such as Nd:YAG [22], Nd:YVO<sub>4</sub> [23], and Nd:GdVO<sub>4</sub> crystals [24], etc. Even though passively

\* Corresponding author. Tel.: +886-35712121; fax: +886-35729134.

E-mail address: [yfchen@cc.nctu.edu.tw](mailto:yfchen@cc.nctu.edu.tw) (Y.F. Chen).

Q-switched Nd:YVO<sub>4</sub> and Nd:GdVO<sub>4</sub> lasers have been demonstrated, their large emission cross-sections lead to the output pulse energy and peak power to be obviously lower than those of Nd:YAG laser. Therefore, so far the pumped sources for passively Q-switched intracavity OPO's are mostly composed of Nd:YAG and Cr<sup>4+</sup>:YAG crystals. The relatively narrow absorption band of Nd:YAG crystal, however, sets stringent requirements on the spectrum of the pump diodes.

Recently, we demonstrated a compact efficient eye-safe OPO to produce 255 mW at 1573 nm by using a nearly hemispherical cavity [25]. In this work we consider the thermal lensing effects to scale up the average output power and peak power at 1573 nm based on a diode-pumped passively Q-switched Nd:YVO<sub>4</sub>/KTP/Cr<sup>4+</sup>:YAG intracavity OPO. The design of the mode-to-pump size ratio is one of the critical issues for a high-power end-pumped laser [26]. The theoretical analysis indicates that the optimum mode-to-pump size ratio for high pump power can be nearly satisfied by controlling the pump size in the previous cavity configuration. With an incident pump power of 14.5 W, the compact intracavity OPO cavity, operating at 58.5 kHz, produces average powers at 1573 nm up to 1.56 W and peak powers higher than 5 kW.

## 2. Experimental setup

Fig. 1 is a schematic of the passively Q-switched intracavity OPO laser. Here a saturable absorber Cr<sup>4+</sup>:YAG is coated as an output coupler of the OPO cavity and a nearly hemispherical cavity is used to enhance the performance of passive

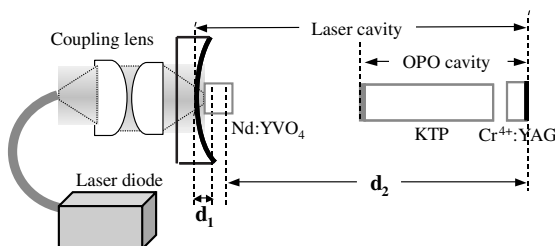


Fig. 1. Schematic of the intracavity OPO pumped by a diode-pumped passively Q-switched Nd:YVO<sub>4</sub>/Cr<sup>4+</sup>:YAG laser.

Q-switching. The active medium was an *a*-cut 0.5 at.% Nd<sup>3+</sup>, 7-mm long Nd:YVO<sub>4</sub> crystal. Both sides of the laser crystal were coated for antireflection at 1064 nm ( $R < 0.2\%$ ). A Nd:YVO<sub>4</sub> crystal with low doping concentration was used to avoid the thermally induced fracture [27]. The laser crystal was wrapped with indium foil and mounted in a water-cooled copper block. The water temperature was maintained at 25 °C. The pump source was a 16-W 808-nm fiber-coupled laser diode with a core diameter of 800 μm and a numerical aperture of 0.2. Focusing lens with 12.5 mm focal length and 92% coupling efficiency was used to re-image the pump beam into the laser crystal. The pump spot radius,  $\omega_p$ , was around 350 μm. The input mirror, M1, was a 50 mm radius-of-curvature concave mirror with antireflection coating at the diode wavelength on the entrance face ( $R < 0.2\%$ ), high-reflection coating at lasing wavelength ( $R > 99.8\%$ ) and high-transmission coating at the diode wavelength on the other surface ( $T > 95\%$ ). Note that the laser crystal was placed very near the input mirror. The OPO cavity was formed by a coated KTP crystal and a coated Cr<sup>4+</sup>:YAG crystal. The 20-mm long KTP crystal was used in type II noncritical phase-matching configuration along the *x*-axis ( $\theta = 90^\circ$  and  $\phi = 0^\circ$ ) to have both a maximum effective nonlinear coefficient and no walk-off between the pump, signal, and idler beams. The KTP crystal was coated to have high reflectivity at the signal wavelength of 1573 nm ( $R > 99.8\%$ ) and high transmission at the pump wavelength of 1064 nm ( $T > 95\%$ ). The other face of the KTP crystal was antireflection coated at 1573 and 1064 nm. The Cr<sup>4+</sup>:YAG crystal has a thickness of 3 mm with 80% initial transmission at 1064 nm. One side of the Cr<sup>4+</sup>:YAG crystal was coated so that it was nominally highly reflecting at 1064 nm ( $R > 99.8\%$ ) and partially reflecting at 1573 nm ( $R_s = 85\%$ ). The remaining side was antireflection coated at 1064 and 1573 nm. The overall Nd:YVO<sub>4</sub> laser cavity length was approximately 55 mm and the OPO cavity length was about 24 mm. As shown in the subsequent analysis, the present cavity length allows mode matching with the pump beam and provides the proper spot size in the saturable absorber.

### 3. Analysis

The thermal lens of a laser crystal always affects the stability of a resonator, especially at a high pump power. An end-pump-induced thermal lens is not a perfect lens, but is rather an aberrated lens. It has been found that the thermally induced diffraction loss at a given pump power is a rapidly increasing function of mode-to-pump ratio. Practically, the optimum mode-to-pump ratio is in the range of about 0.6–1.0 when the incident pump power is greater than 5 W. For a fiber-coupled laser diode, the thermal lens can be given by [28]

$$\frac{1}{f_{th}} = \int_0^l \frac{\xi P_{in}}{2\pi K_c} \frac{\alpha e^{-\alpha z}}{1 - e^{-\alpha l}} \times \frac{[dn/dT + (n - 1)\alpha_T]}{\omega_p^2 \left\{ 1 + \left[ \lambda_p M_p^2 (z - z_0) / \pi n \omega_p^2 \right]^2 \right\}} dz, \quad (1)$$

where  $\xi$  is the fractional thermal loading,  $K_c$  is the thermal conductivity,  $P_{in}$  is the incident pump power,  $n$  is the refractive indices along the  $c$ -axis of the Nd:YVO<sub>4</sub> crystal,  $dn/dT$  is the thermal-optic coefficients of  $n$ ,  $\alpha_T$  is the thermal expansion coefficient along the  $a$ -axis,  $l$  is the crystal length,  $\omega_p$  is the radius at the waist,  $\lambda_p$  is the pump wavelength,  $M_p^2$  is the pump beam quality factor, and  $z_0$  is focal plane of the pump beam in the active medium. The first and second terms in the parenthesis of Eq. (1) arise from the thermal dispersion and the axial strain, respectively.

Considering the thermal lensing effect on the laser crystal, the mode beam radii  $\omega_1$  on the laser crystal and  $\omega_2$  on the saturable absorber can be given by [29]

$$\omega_i = \sqrt{\frac{\lambda L}{\pi}} \sqrt{\frac{g_j}{g_i(1 - g_1 g_2)}} \quad i, j = 1, 2; \quad i \neq j, \quad (2)$$

where  $g_1 = 1 - (d_1 + d_2^*)/\rho_1 - d_2^*(1 - d_1/\rho_1)/f_{th}$ ,  $g_2 = 1 - d_1/f_{th}$ ,  $L = d_1 + d_2^* - d_1 d_2^*/f_{th}$ ,  $d_2^* = d_2 + l_s(1/n_s - 1) + l_{KTP}(1/n_{KTP} - 1)$ ,  $\lambda$  is the lasing wavelength,  $\rho_1$  is the radius of curvature of the input mirror,  $d_1$  and  $d_2$  are the distances between the cavity mirrors and the principal planes of the laser crystal,  $n_s$  and  $n_{KTP}$  are, respectively, the refractive indices of the saturable absorber and the KTP crystal, and  $l_s$  and  $l_{KTP}$  are, respectively, the

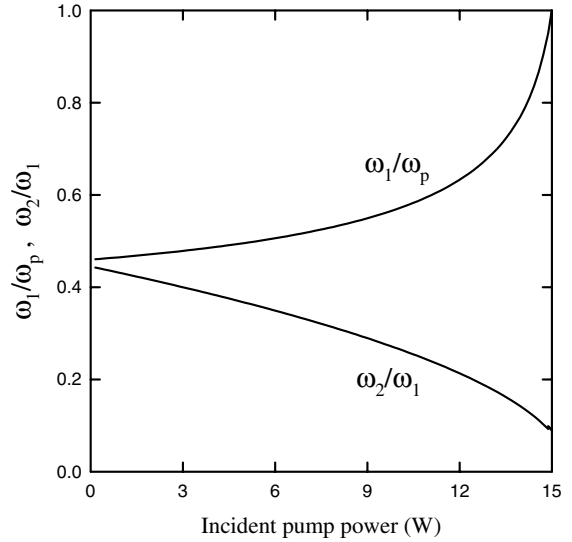


Fig. 2. Calculation results for the dependence of the mode size ratios  $\omega_1/\omega_p$  and  $\omega_2/\omega_1$  on the pump power for the present cavity configuration.

lengths of the saturable absorber and the KTP crystal. Note that the principal planes of the thermal lens can be approximated to be located inside the laser crystal at a distance  $h = l/2n$  [29].

With Eqs. (1) and (2), the dependence of the mode size ratios  $\omega_1/\omega_p$  and  $\omega_2/\omega_1$  on the pump power for the present cavity configuration was calculated and shown in Fig. 2. The parameters used in the calculation are as follows:  $\xi = 0.24$ ,  $K_c = 0.0523$  W/K cm,  $\omega_p = 0.35$  mm,  $M_p^2 \approx 310$ ,  $d_1 = 2$  mm,  $d_2 = 48$  mm,  $\rho_1 = 50$  mm,  $n = 2.165$ ,  $n_s = 1.82$ ,  $n_{KTP} = 1.745$ ,  $l = 7$  mm,  $l_{KTP} = 20$  mm,  $l_s = 3$  mm,  $dn_c/dT = 3.0 \times 10^{-6}$  K<sup>-1</sup>, and  $\alpha_T = 4.43 \times 10^{-6}$  K<sup>-1</sup>. It is clear from Fig. 2 that mode-to-pump size ratio  $\omega_1/\omega_p$  is around 0.6–1.0 for pump powers within 10–15 W, leading to optimal mode matching [26]. On the other hand, the ratio of the mode size in the saturable absorber and in the gain medium  $\omega_2/\omega_1$  can be in the range of 0.1–0.3, satisfying the criterion for good passively Q-switching [30,31].

### 4. Experimental results

Fig. 3 shows the average output power at 1573 nm with respect to the incident pump power. For

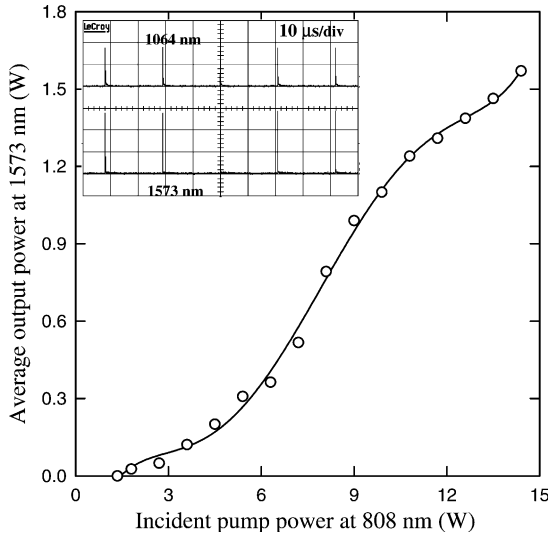


Fig. 3. Dependence of the average output power at 1573 nm on the incident pump power. An oscilloscope trace of a train of the signal pulses is shown in the inset.

all pump powers the beam quality  $M^2$  factor was found to be less than 1.3. The average output power reached 1.56 W at an incident pump power of 14.5 W. The conversion efficient from diode laser input power to OPO signal output power was 10.8%. To the best of our knowledge, this is highest efficiency for average power conversion. The pulse temporal behavior at 1064 and 1573 nm was recorded by a LeCroy 9362 digital oscilloscope (500 MHz bandwidth) with a fast germanium photodiode. An oscilloscope trace of a train of the signal pulses is shown in the inset of Fig. 3. The pulse-to-pulse amplitude fluctuation was found to be within  $\pm 10\%$ .

Fig. 4 depicts the pulse repetition rate and the pulse energy at 1573 nm versus the incident pump power. It is seen that the pulse repetition rate is proportional to the incident pump power and up to 58.5 kHz at an incident pump power of 14.5 W. On the other hand, the pulse energy initially increases with pump power, and is almost saturated beyond 10 W of the incident pump power. The saturation of the pulse energy implies that the criterion for good passively Q-switching was entirely fulfilled. From the analysis of the coupled rate-equation, the criterion for good passively Q-switching is given by [32]

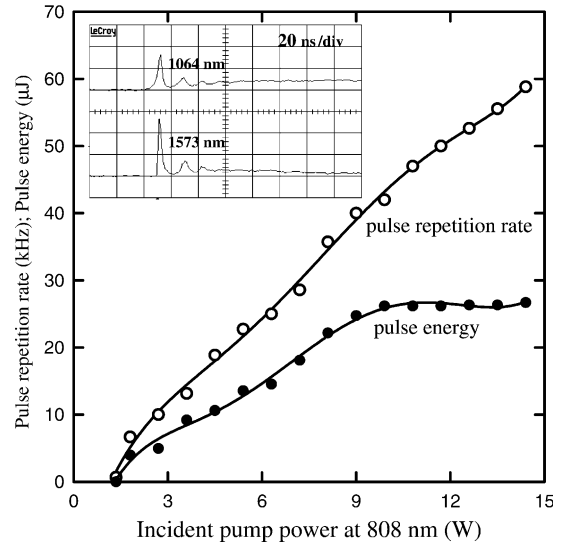


Fig. 4. Dependence of the pulse repetition rate and the pulse energy at 1573 nm on the incident pump power. A typical temporal shape for the laser and signal pulses is shown in the inset.

$$\frac{\ln\left(\frac{1}{T_0}\right)}{\ln\left(\frac{1}{T_0}\right) + \ln\left(\frac{1}{R}\right) + L} \frac{\sigma_{gs}}{\sigma} \frac{A}{A_s} \gg \frac{\gamma}{1-\beta}, \quad (3)$$

where  $T_0$  is the initial transmission of the saturable absorber,  $A/A_s$  is the ratio of the effective area in the gain medium and in the saturable absorber,  $R$  is the reflectivity of the output mirror,  $L$  is the nonsaturable intracavity round-trip dissipative optical loss,  $\sigma_{gs}$  is the ground-state absorption cross-section of the saturable absorber,  $\sigma$  is the stimulated emission cross-section of the gain medium,  $\gamma$  is the inversion reduction factor with a value between 0 and 2 as discussed in [33], and  $\beta$  is the ratio of the excited-state absorption cross-section to that of the ground-state absorption in the saturable absorber. Since the  $\sigma$  value of the Nd:YVO<sub>4</sub> crystal ( $25 \times 10^{-19} \text{ cm}^2$ ) is comparable to the  $\sigma_{gs}$  value of the Cr<sup>4+</sup>:YAG crystal ( $\sim (20 \pm 5) \times 10^{-19} \text{ cm}^2$  [34]), the ratio  $A/A_s = (\omega_1/\omega_2)^2$  generally needs to be greater than 10 for good passively Q-switching. As seen in Fig. 2, this criterion can be satisfied in the present cavity for pump power higher than 10 W. In other words, the experimental result consists very well with the theoretical analysis. A typical temporal shape for the laser and signal pulses is shown

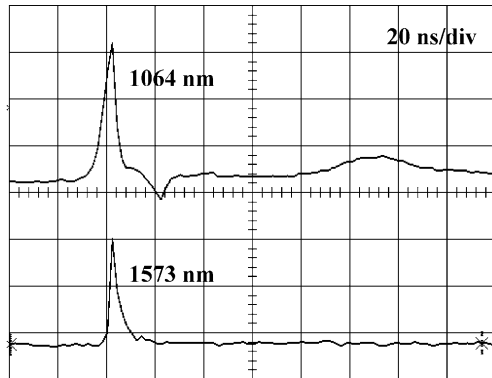


Fig. 5. Typical temporal shapes for the laser and signal pulses with a signal reflectivity of 70% on the output coupler.

in the inset of Fig. 4. It can be seen that the several satellite peaks accompany the main pulse whose pulse width is approximately 2.5 ns. Although the present output coupler reflectivity ( $R_s = 85\%$ ) can lead to higher conversion efficiency, the stored energy is not fully extracted in a single output pulse. Since the remaining energy is sufficient to evolve the pump field, the OPO threshold can be reached again and a second signal pulse is produced. The energy in the satellites is about 30–40% of the total output energy. The output energy of the main pulse is estimated to be in the order of 15  $\mu\text{J}$  at the pump power higher than 10 W. Therefore, the overall peak power can be higher than 5 kW. To produce a single pulse output, the OPO output reflectivity needs to be reduced to  $<75\%$ . As shown in Fig. 5, a single pulse can be generated with a signal reflectivity of 70% on the output coupler. Experimental results reveal that the maximum conversion efficiency can be obtained with an output coupler of 85–90% at the sacrifice of peak power. If the high peak power is desired, the output reflectivity needs to be around 60–70%.

## 5. Summary

In summary, a high-power efficient diode-pumped passively Q-switched Nd:YVO<sub>4</sub>/KTP/Cr<sup>4+</sup>:YAG eye-safe laser has been demonstrated by using a saturable absorber Cr<sup>4+</sup>:YAG was coated as an output coupler of the OPO cavity to

enhance the performance of passive Q-switching. Considering the thermal lensing effects, the cavity length was designed to allow mode matching with the pump beam and to provide the proper spot size in the saturable absorber. Consequently, the average output power at 1573 nm can amount to 1.56 W with a pulse repetition rate of 58.5 kHz and the peak power  $>5$  kW at an incident pump power of 14.5 W.

## References

- [1] R.C. Stoneman, L. Esterowitz, in: Proceedings of the Conference on Advanced Solid State Lasers, Optical Society of America, Washington, DC, 1990, p. 176, paper WC5-2.
- [2] P.F. Moulton, IEEE J. Quantum Electron. 21 (1985) 1582.
- [3] P.F. Moulton, A. Mooradian, Appl. Phys. Lett. 35 (1979) 838.
- [4] S. Kück, K. Petermann, U. Pohlmann, G. Huber, Phys. Rev. B 51 (1995) 17323.
- [5] A. Sennaroglu, Prog. Quantum Electron. 26 (2002) 287.
- [6] B. Schmaul, G. Huber, R. Clausen, B. Chai, P. LikamWa, M. Bass, Appl. Phys. Lett. 62 (1993) 541.
- [7] M.V. Kuleshov, A.A. Lagatsky, A.V. Podlipensky, V.P. Mikhailov, A.A. Kornienko, E.B. Dunina, S. Hartung, G. Huber, J. Opt. Soc. Am. B 15 (1998) 1205.
- [8] I. Sokólska, E. Heumann, S. Kück, T. Lukasiewicz, Appl. Phys. B 71 (2000) 893.
- [9] A. Diening, P.E.-A. Möbert, G. Huber, J. Appl. Phys. 84 (1998) 5900.
- [10] S. Taccheo, P. Laporta, S. Longhi, O. Svelto, C. Svelto, Appl. Phys. B 63 (1996) 425.
- [11] K.V. Yumashev, I.A. Denisov, N.N. Posnov, V.P. Mikhailov, R. Moncorgé, D. Vivien, B. Ferrand, Y. Guyot, J. Opt. Soc. Am. B 16 (1999) 2189.
- [12] K. Spariosu, R.D. Stultz, M. Birnbaum, T.H. Allik, J.A. Hutchinson, Appl. Phys. Lett. 62 (1993) 2763.
- [13] R.D. Stultz, M.B. Camargo, M. Birnbaum, J. Appl. Phys. 78 (1995) 2959.
- [14] R.D. Stultz, M.B. Camargo, M. Lawler, D. Rockafellow, M. Birnbaum, in: W.R. Bosenberg, M.M. Fejer (Eds.), Advanced Solid State Lasers, OSA Trends in Optics and Photonics Series, vol. 19, Optical Society of America, Washington, DC, 1998, p. 155.
- [15] R.D. Stultz, M.B. Camargo, S.T. Montgomery, M. Birnbaum, K. Spariosu, Appl. Phys. Lett. 64 (1994) 948.
- [16] M. Birnbaum, M.B. Camargo, S. Lee, F. Unlu, R.D. Stultz, in: C.R. Pollock, W.R. Bosenberg (Eds.), Advanced Solid State Lasers, OSA Trends in Optics and Photonics Series, vol. 10, Optical Society of America, Washington, DC, 1997, p. 148.
- [17] R. Fluck, R. Häring, R. Paschotta, E. Gini, H. Melchior, U. Keller, Appl. Phys. Lett. 72 (1998) 3273.

- [18] J. Falk, J.M. Yarborough, E.O. Ammann, *IEEE J. Quantum Electron.* 7 (1971) 359.
- [19] R.S. Conroy, C.F. Rae, G.J. Friel, M.H. Dunn, B.D. Sinclair, J.M. Ley, *Opt. Lett.* 23 (1998) 1348.
- [20] A.R. Geiger, H. Hemmati, W.H. Farr, N.S. Prasad, *Opt. Lett.* 21 (1996) 201.
- [21] O.B. Jensen, T. Skettrup, O.B. Petersen, M.B. Larsen, *J. Opt. A: Pure Appl. Opt.* 4 (2002) 190.
- [22] J.J. Zayhowski, C. Dill III, *Opt. Lett.* 19 (1994) 1427.
- [23] Y.X. Bai, N. Wu, J. Zhang, J.Q. Li, S.Q. Li, J. Xu, P.Z. Deng, *Appl. Opt.* 36 (1997) 2468.
- [24] C. Li, J. Song, D. Shen, N.S. Kim, J. Lu, K. Ueda, *Appl. Phys. B* 70 (2000) 471.
- [25] Y.F. Chen, S.W. Chen, Y.C. Chen, Y.P. Lan, S.W. Tsai, *Appl. Phys. B* 77 (2003) 493.
- [26] Y.F. Chen, T.M. Huang, C.F. Kao, C.L. Wang, S.C. Wang, *IEEE J. Quantum Electron.* 33 (1997) 1424.
- [27] Y.F. Chen, *IEEE J. Quantum Electron.* 35 (1999) 234.
- [28] Y.F. Chen, T.M. Huang, C.C. Liao, Y.P. Lan, S.C. Wang, *IEEE Photon. Technol. Lett.* 11 (1997) 1241.
- [29] N. Hodgson, H. Weber, *Optical Resonators*, Springer-Verlag, Berlin, 1997.
- [30] A.E. Siegman, *Laser*, University Science, Mill Valley, CA, 1986, pp. 1024 and 1012.
- [31] Y.F. Chen, S.W. Tsai, *IEEE J. Quantum Electron.* 37 (2001) 586.
- [32] Y.F. Chen, Y.P. Lan, H.L. Chang, *J. Quantum Electron.* 37 (2001) 462.
- [33] J.J. Degnan, D.B. Coyle, R.B. Kay, *IEEE J. Quantum Electron.* 34 (1998) 887.
- [34] G. Xiao, J.H. Lim, S. Ynag, E.V. Stryland, M. Bass, L. Weichman, *IEEE J. Quantum Electron.* 35 (1997) 1086.